Effective field theory of the Majorana dark matter*

Hua-Yong Han(韩华勇)[1;1)] Hong-Yan Wu(吴红彦)[2,3;2)] Si-Bo Zheng(郑思波)[2;3)]

[1]CAS Key Laboratory of Theoretical Physics, Institute of Theoretical Physics, Chinese Academy of Sciences, Beijing 100190, China
[2]Department of Physics, Chongqing University, Chongqing 401331, China
[3]School of Physics, Peking University, Beijing 100871, China

Abstract: We revisit the thermal Majorana dark matter from the viewpoint of the minimal effective field theory. In this framework, analytical results for dark matter annihilation into Standard Model particles are derived. The dark matter parameter space, subject to the latest LUX, PandaX-II and Xenon-1T limits, is presented in a model-independent way. Applications to the singlet-doublet and MSSM are presented.

Keywords: dark matter, effective field theory, Majorana

PACS: 95.35.+d, 12.60.-i **DOI:** 10.1088/1674-1137/43/4/043103

1 Introduction

From the viewpoint of standard cosmology, cold dark matter (DM) is a neutral particle beyond the Standard Model (SM), which has not been observed in either particle astrophysics or collider experiments. Due to its electrically neutral property, it is natural to consider DM as a Majorana fermion. The Majorana DM appears in a number of well known models, such as the neutralino [1], singlet-doublet [2-9], Higgs-portal [10-13] and Z-portal [14-19] DM.

For the Majorana DM, the effective Lagrangian at the weak scale is described by,

$$\mathcal{L} = \mathcal{L}_{\rm SM} + \mathcal{L}_{\rm dark}(\chi, \cdots), \tag{1}$$

where the SM Lagrangian $\mathcal{L}_{\rm SM}$ contains the interactions between DM mediators h and Z and SM particles,

$$\mathcal{L}_{\rm SM} \supset \frac{h}{\upsilon_{\rm EW}}\left(\sum_f m_f\bar{\psi}_f\psi_f + 2m_w^2 W_\mu^+ W^{-\mu} + m_z^2 Z^\mu Z_\mu\right) + Z_\mu\sum_f \bar{\psi}_f\gamma^\mu(g_V - g_A\gamma_5)\psi_f + \cdots \tag{2}$$

with

$$g_V = \frac{g}{\cos\theta_W}\left(\frac{T_{3f}}{2} - Q_f\sin^2\theta_W\right),\ g_A = \frac{g}{\cos\theta_W}\left(\frac{T_{3f}}{2}\right). \tag{3}$$

Here, the weak scale $\upsilon_{\rm EW}$=246 GeV, $g \simeq 0.65$ is the gauge coupling of the $SU(2)_L$ group, θ_W denotes the weak mixing angle, and Q_f is the electric charge, with $T_{3f} = +(-)\frac{1}{2}$ for the up (down)-type SM fermion, respectively.

Moreover, $\mathcal{L}_{\rm dark}$ in Eq. (1) generally contains the interactions between Majorana DM (in 4-component notation) and SM mediators[4)],

$$\mathcal{L}_{\rm dark}(\chi, \cdots) \supset c_h h\bar{\chi}\chi + c_z Z^\mu\bar{\chi}\gamma_\mu\gamma_5\chi + \cdots, \tag{4}$$

The c_h and c_z interaction terms constitute the minimal framework from the perspective of the effective field theory, where higher-dimensional operators [20], responsible for the obvious gauge invariance of Eq. (4), should be taken into account. We refer to $\mathcal{L}_{\rm dark}$ in Eq. (4) as the "minimal" effective field theory.

New physical particles beyond the minimal effective field theory impose diverse effects. If they are decoupled, their net effects are recorded in parameters c_h and c_z in Eq. (4). Conversely, if they are not, they should be included in Eq. (2) or Eq. (4), which either play the role of the new mediator between DM and SM sectors, or contribute to new DM annihilation final states if they are kinetically allowed. In the former case, the Lagrangians in Eq. (2) and Eq. (4) contain all possible contributions to DM annihilation and DM scattering cross sections. In the latter case, new particles with a mass of the order of the weak scale yield a small number of new Feynman diagrams for these cross sections. When the number of new

Received 24 September 2018, Revised 14 January 2019, Published online 4 March 2019

* Supported by National Natural Science Foundation of China (11775039) and Postdoctoral Science Foundation of China (2017M611008)

1) E-mail: han@itp.ac.cn
2) E-mail: hongyanwu@pku.edu.cn
3) E-mail: sibozheng.zju@gmail.com, corresponding author

4) Note, there is no vector coupling between Majorana DM and Z boson.

particles is large, the numerical treatment is more viable than an analytical one. Nevertheless, it is only the analytical treatment that can clearly show the ingredients required for recognizing the future signatures of DM direct detection, which is the main motivation for this study.

The rest of the paper is organized as follows. Section 2 is devoted to an analytical derivation of DM annihilation into the SM final states in the minimal framework. We will compare our results with numerical calculations. In Section 3, we show the parameter space subject to the latest DM direct detection limits in a model-independent way. In Section 4, we apply our method to the singlet-doublet and the minimal supersymmetric standard model (MSSM). Finally, we conclude in Section 5.

2 Relic density

According to the effective Lagrangian in Eq. (1), DM can annihilate into the SM final states such as $f\bar{f}$, ZZ, WW, Zh and hh through the SM mediators h and/or Z. In order to calculate the DM relic density, we first derive the thermally averaged cross section $\langle\sigma v_\chi\rangle$. The Feynman diagrams responsible are shown in Fig. 1. Although the Feynman diagrams similar to Fig. 1 have already been discussed in a more complicated context such as the neutralino DM [21], a concrete analytical expression for the DM annihilation cross section is only viable in some simplified situations, such as the minimal framework discussed here.

As is well known, the DM annihilation cross section times the DM relative velocity v_χ can be expanded in the standard way,

$$\sigma v_\chi = a + b v_\chi^2 + O(v_\chi^4). \tag{5}$$

In Table 1 , we introduce the coefficients a and b for the various SM final states of Fig. 1. Direct evaluation yields

$$a_{ff} = \frac{2N_c c_z^2 r_{f\chi} g_A^2 m_f^2}{\pi m_Z^4}, \tag{6}$$

$$a_{zz} = \frac{4c_z^4 r_{z\chi}\left(m_\chi^2 - m_Z^2\right)}{\pi\left(m_Z^2 - 2m_\chi^2\right)^2}, \tag{7}$$

$$a_{zh} = \frac{c_z^2 r_{\chi zh}^3 m_\chi^2}{64\pi v_{\rm EW}^2 m_Z^2}, \tag{8}$$

and

$$b_{ff} = \frac{N_c c_h^2 m_f^2 r_{f\chi}\left(m_\chi^2 - m_f^2\right)}{2\pi v_{\rm EW}^2\left(m_h^2 - 4m_\chi^2\right)^2} + \frac{N_c c_z^2 g_A^2 m_f^2\left(5m_f^2 - 4m_\chi^2\right)}{4\pi r_{f\chi} m_\chi^2 m_Z^4} + \frac{N_c c_z^2 r_{f\chi}\left(m_f^2(g_V^2 - 2g_A^2) + 2m_\chi^2(g_V^2 + g_A^2)\right)}{3\pi\left(m_Z^2 - 4m_\chi^2\right)^2}, \tag{9}$$

$$b_{\rm ww} = \frac{c_h^2 r_{w\chi}\left(-4m_W^2 m_\chi^2 + 4m_\chi^4 + 3m_W^4\right)}{4\pi v_{\rm EW}^2\left(m_h^2 - 4m_\chi^2\right)^2} + \frac{c_z^2 r_{w\chi} g^2 \cos^2\theta_W\left(-17m_W^4 m_\chi^2 + 16m_\chi^4 m_w^2 - 3m_W^6 + 4m_\chi^6\right)}{6\pi m_W^4\left(m_Z^2 - 4m_\chi^2\right)^2}, \tag{10}$$

$$b_{zz} = \frac{c_h^2 r_{z\chi}\left(-4m_Z^2 m_\chi^2 + 4m_\chi^4 + 3m_Z^4\right)}{8\pi v_{\rm EW}^2\left(m_h^2 - 4m_\chi^2\right)^2} + \frac{2c_h c_z^2 r_{z\chi} m_\chi\left(-9m_Z^4 m_\chi^2 + 12m_Z^2 m_\chi^4 - 8m_\chi^6 + 2m_Z^6\right)}{3\pi v_{\rm EW}\left(m_h^2 - 4m_\chi^2\right)\left(m_Z^3 - 2m_Z m_\chi^2\right)^2} + \frac{c_z^4 r_{z\chi}\left(-118m_Z^8 m_\chi^2 + 172m_Z^6 m_\chi^4 + 32m_Z^4 m_\chi^6 - 192m_Z^2 m_\chi^8 + 128m_\chi^{10} + 23m_Z^{10}\right)}{6\pi\left(m_Z^3 - 2m_Z m_\chi^2\right)^4}, \tag{11}$$

$$b_{hh} = \frac{9c_h^2 m_h^4 r_{h\chi}}{32\pi v_{\rm EW}^2\left(m_h^2 - 4m_\chi^2\right)^2} + \frac{c_h^3 m_h^2 r_{h\chi} m_\chi\left(2m_h^2 - 5m_\chi^2\right)}{2\pi v_{\rm EW}\left(m_h^2 - 4m_\chi^2\right)\left(m_h^2 - 2m_\chi^2\right)^2} + \frac{2c_h^4 r_{h\chi} m_\chi^2\left(-8m_h^2 m_\chi^2 + 9m_\chi^4 + 2m_h^4\right)}{3\pi\left(m_h^2 - 2m_\chi^2\right)^4}, \tag{12}$$

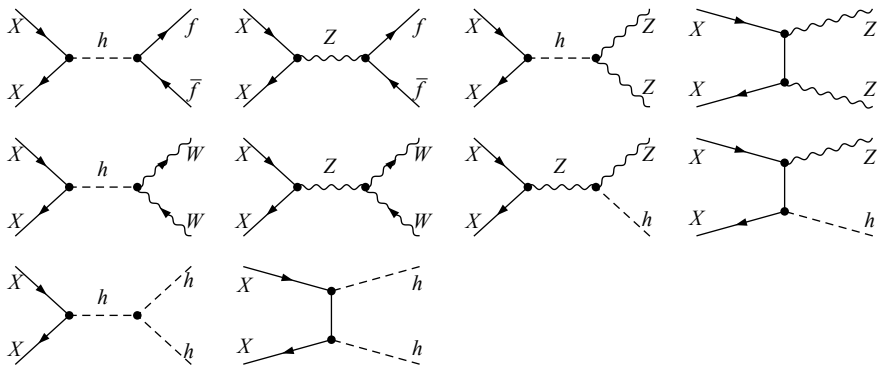

Fig. 1. Feynman diagrams for DM annihilation into the SM final states.

$$b_{zh}=\frac{c_z^2 r_{\chi zh}}{768\pi v_{\rm EW}^2 m_\chi^2 m_Z^2\left(m_Z^2-4m_\chi^2\right)^2}\left[\left(4m_Z^6\left(5m_h^2+59m_\chi^2\right)-2m_Z^4\left(5m_h^4+74m_h^2m_\chi^2+344m_\chi^4\right)+96m_\chi^2m_Z^2\left(m_h^4-m_h^2m_\chi^2+14m_\chi^4\right)\right.\right.$$
$$\left.-192m_\chi^4\left(m_h^4-5m_h^2m_\chi^2+4m_\chi^4\right)-10m_Z^8\right)\Big]+\frac{c_h c_z^2 r_{\chi zh}}{12\pi v_{\rm EW} m_\chi m_Z^2\left(4m_\chi^2-m_Z^2\right)\left(m_h^2-4m_\chi^2+m_Z^2\right)^2}\left[\left(2m_Z^6\left(m_h^2-9m_\chi^2\right)\right.\right.$$
$$\left.-2m_\chi^2\left(m_h^2-4m_\chi^2\right)^3-m_Z^4\left(m_h^4+14m_h^2m_\chi^2-104m_\chi^4\right)+2m_\chi^2m_Z^2\left(m_h^4+8m_h^2m_\chi^2-48m_\chi^4\right)-m_Z^8\right)\Big]$$
$$+\frac{c_h^2c_z^2r_{\chi zh}}{768\pi m_\chi^2m_Z^2\left(m_h^2-4m_\chi^2+m_Z^2\right)^4}\left[m_Z^{10}+2m_Z^6\left(3m_h^4+16m_\chi^4\right)+4m_Z^8\left(m_\chi^2-m_h^2\right)\right.$$
$$\left.-4m_Z^4\left(m_h^2-4m_\chi^2\right)^2\left(m_h^2+10m_\chi^2\right)+4m_\chi^2\left(m_h^2-4m_\chi^2\right)^4+m_Z^2\left(m_h^2-4m_\chi^2\right)^2\left(m_h^4+8m_h^2m_\chi^2+80m_\chi^4\right)\right] \quad (13)$$

Table 1. Coefficients of the σv_χ expansion into the individual SM final states.

channel	a	b
$f\bar{f}$	a_{ff}	b_{ff}
ZZ	a_{zz}	b_{zz}
W^+W^-	–	$b_{\rm ww}$
hh	–	b_{hh}
Zh	a_{zh}	b_{zh}

where $N_c=1(3)$ for the SM lepton (quark), and m_χ refers to the DM mass. Functionals r_{ij} and $r_{\chi ij}$ are defined respectively as

$$r_{ij}=\sqrt{1-m_i^2/m_j^2},$$
$$r_{\chi ij}=\sqrt{m_i^4-2m_i^2(m_j^2+4m_\chi^2)+(m_j^2-4m_\chi^2)^2}/m_\chi^2.$$

A few comments are in order regarding our results. First, in the case $c_h\to 0$, both a_{ff} and a_{zz} in Eq. (6)-Eq. (7) coincide with the results for the Z portal [15, 19], but b_{ff} and b_{zz} in [19] are both two times that in Eq. (9) and Eq. (11), respectively. Second, in the case $c_z\to 0$, all coefficients a in Eq. (6)-Eq. (8) disappear, the same as in the Higgs portal, and our b_{ff} in Eq. (9) and b_{zz} and b_{hh} (the c_h^2-term) are in agreement with the results of [13] and [10], respectively. Third, when both c_z and c_h are non-zero, interference effects occur in b_{zz} and b_{zh}, which are explicitly shown. These interference effects can be neglected except in some particular DM mass range between m_z and m_h, where it is not small relative to the other contributions. Finally, we have also included the SM Higgs self-interaction contribution to b_{hh} in Eq. (12). We verified that our results agree with the numerical calculations obtained using the code MicrOMEGAs [22], with a deviation of at most 10%-15% in the estimate of the DM relic density.

3 Direct detection

The interactions in Eq. (4) yield both spin-dependent (SD) and spin-independent (SI) effective couplings between DM and SM nucleons. In particular, the Yukawa coupling constants c_h and c_z control the SI and SD scattering cross sections, respectively, which are given by [1, 23],

$$\sigma_{\rm SI}\simeq c_h^2\times(2.11\times10^3{\rm zb}),$$
$$\sigma_{\rm SD}^p\simeq c_z^2\times(1.17\times10^9{\rm zb}),$$
$$\sigma_{\rm SD}^n\simeq c_z^2\times(8.97\times10^8{\rm zb}). \quad (14)$$

Here, the nuclear form factors have been chosen as in [24]. The approximations for $\sigma_{\rm SI}$ and $\sigma_{\rm SD}$ are always valid for the DM mass m_χ above a few times $m_{p,n}$.

In Fig. 2 , we show the parameter space of the DM relic density $\Omega_{\rm DM}h^2=0.1199\pm0.0027$ [25] in the two-parameter plane c_h and c_z, with the contours referring to DM masses in units of GeV. We also draw contours from the latest PandaX-II [26], Xenon-1T [27] and LUX 2016 [28] limits. Parameter regions above the color lines, or on the right-hand side of the blue line, are excluded, from which we find that model-independent exclusion limit for the DM mass is about ~155 GeV. Only a small region

$$0\leqslant|c_z|\leqslant0.018,\quad 0\leqslant|c_h|\leqslant0.06 \quad (15)$$

is left for future tests. If this region is excluded by future experimental limits, we can draw the conclusion that either a new particle(s) is required at the weak scale, or that the simplified Majorana DM models are disfavored. In what follows, we will discuss the implication of our results on a few simplified models.

The parameter space for the coupling of c_z and c_h (alternatively the DM mass range), as given by Eq. (15), is not affected by other constraints such as the mono-jet limit [29-31] at the LHC, or the constraint on the DM annihilation cross section $\sigma(\chi\chi\to\gamma\gamma)$ at Fermi-LAT [32-34]. The mono-jet constraint is sensitive to parameter c_z only for a DM mass $m_\chi<M_Z/2$ in our situation, which excludes a DM mass below ~50 GeV for $c_z=1.0$, see e.g. [31]. This implies that the surviving DM mass range referred to in Eq. (15), is not sensitive to the present mono-jet limit. On the other hand, the Fermi-LAT constraint on

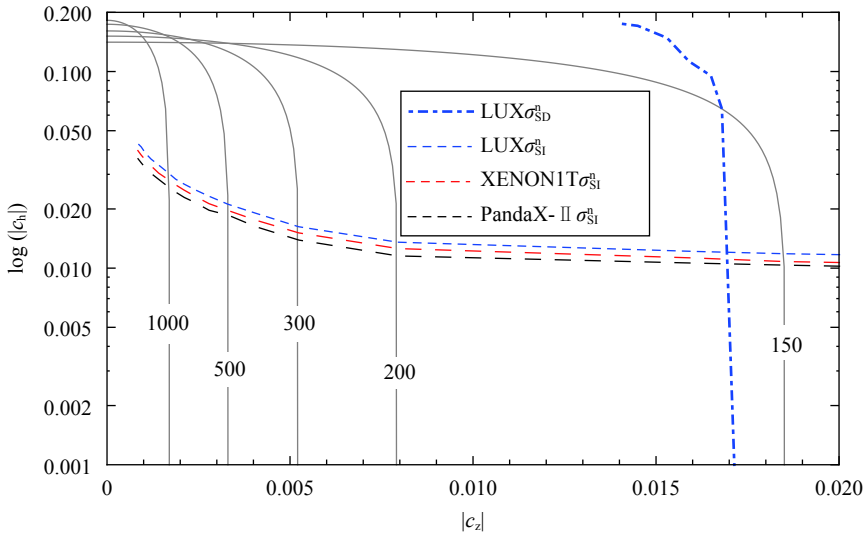

Fig. 2. (color online) Parameter space of the DM relic density in the two-parameter plane c_h and c_z subject to the latest PandaX-II [26] (green), Xenon-1T [27] (red), and LUX 2016 [28] (blue) limits. The DM masses (in units of GeV) referring to each contour are drawn for clarity, which implies that the model-independent exclusion limit for the DM mass is about ~155 GeV.

the γ spectrum is sensitive to both c_z and c_h for a DM mass below ~500 GeV, where the Feynman diagram for $\sigma(\chi\chi \to h/Z \to \gamma\gamma)$ is dominated by the top, bottom fermion loop and W boson loop. As expected, there is a peak in the γ spectrum that appears for a DM mass close to half of the mediator mass, i.e, $M_h/2$ or $M_Z/2$ in our case. When the DM mass, such as that corresponding to Eq. (15), obviously deviates from the pole masses above, the Fermi-LAT constraint is weak as well.

4 Applications

4.1 Singlet-doublet dark matter

This model contains two fermion doublets $L' = (l'^0, l^-)^T$, $L = (l^+, l^0)^T$ and a fermion singlet ψ_s. The dark sector Lagrangian $\mathcal{L}_{\rm dark}$ reads as [2-4],

$$\begin{aligned}\mathcal{L}_{\rm dark} =& \frac{i}{2}\left(\bar{\psi}_s\sigma^\mu\partial_\mu\psi_s + \bar{L}'\sigma^\mu\partial_\mu L' + \bar{L}\sigma^\mu\partial_\mu L\right)\\ &+\left(-y_1 L' H\psi_s - y_2\bar{L}\bar{\psi}_s H + \text{H.c}\right)\\ &-\frac{m_{\psi_s}}{2}\psi_s\psi_s - m_D L' L,\end{aligned} \tag{16}$$

where m_s, m_D and $y_{1,2}$ are the mass and Yukawa coupling parameters, respectively. H denotes the SM Higgs doublet. In the basis (ψ_s, l'^0, l^0) the symmetric mass matrix for neutral fermions is given by,

$$M_\chi = \begin{pmatrix} m_s & \frac{y_1 v_{\rm EW}}{\sqrt{2}} & \frac{y_2 v_{\rm EW}}{\sqrt{2}} \\ * & 0 & m_D \\ * & * & 0 \end{pmatrix}. \tag{17}$$

This model is similar to the neutralino sector of the next-to-minimal supersymmetric model (NMSSM) where bino and wino components are both decoupled. Imposing the decoupling limit $m_D >> m_s, v_{\rm EW}$ on the dark sector yields only a light singlet-like DM with mass $m_\chi \simeq m_s$. With this limit, the effective couplings $c_{h\bar{\chi}\chi}$ and $c_{z\bar{\chi}\chi}$ reduce to, respectively [7],

$$\begin{aligned} c_{h\bar{\chi}\chi} &\simeq -\frac{v_{\rm EW}}{m_D}\left(2y_1 y_2 + (y_1^2 + y_2^2)\frac{m_\chi}{m_D}\right),\\ c_{z\bar{\chi}\chi} &\simeq \frac{1}{2}\frac{v_{\rm EW}}{m_D}\frac{m_Z}{m_D}(y_1^2 - y_2^2)\left(1 - \frac{m_\chi^2}{m_D^2}\right). \end{aligned} \tag{18}$$

Note that $|c_z|$ and $|c_h|$ are both unchanged under the exchange $y_1 \leftrightarrow y_2$. Since the parameter ranges in Eq. (15) favor a larger value of $|c_h|$ relative to $|c_z|$, this implies that the product $y_1 y_2$ in Eq. (18) should be at most of the order of m_χ/m_D. Otherwise, $|c_h|$ at the crossing points with the contours of the DM relic density would be too large with respect to the direct detection limits, as shown in Fig. 2.

In Fig. 3 , we show the contours of the DM mass projected on the plane $c_h - c_z$ for $y_1 = -3$ and $y_2 = 0.1$, where the condition that the DM mass $m_\chi \simeq m_s$ should be at least an order of magnitude smaller than m_D has been imposed. The crossing points with the contours of the DM relic density are indeed beneath the DM direct detection limits for the DM mass range between 200 GeV and 600 GeV. When the magnitude of y_1 is tuned to be smaller than 2, these viable crossing points disappear.

4.2 MSSM

We now discuss the application to MSSM with decoupling mass spectrum, in which all supersymmetric particles, except the lightest neutralino, are decoupled

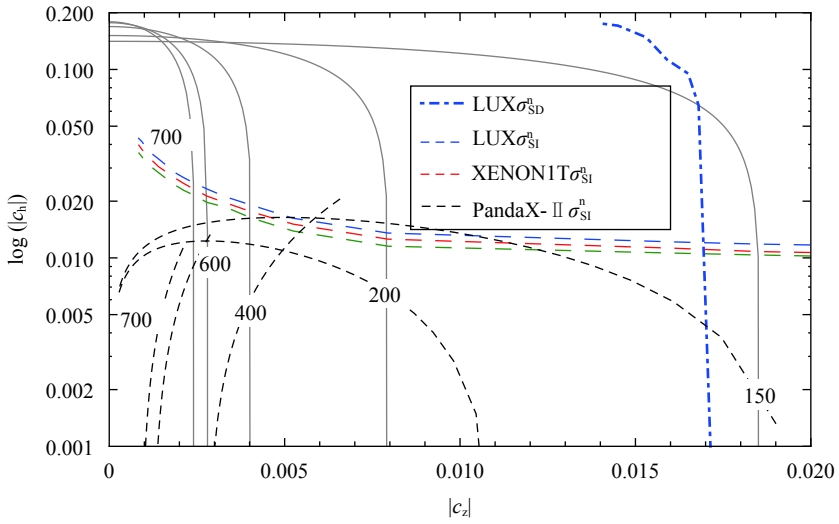

Fig. 3. (color online) Contours of the DM mass in dotted lines projected on the plane $c_h - c_z$ for $y_1 = -3$ and $y_2 = 0.1$. Contours of the DM relic density and color lines are the same as in Fig. 2. We have imposed the condition that the DM mass m_χ should be at least an order of magnitude smaller than m_D.

from the weak scale. The symmetric neutralino mass matrix M_χ under the gauge eigenstates $(\tilde{B}^0, \tilde{W}^0, \tilde{H}_d^0, \tilde{H}_u^0)$ is given by,

$$M_\chi = \begin{pmatrix} M_1 & 0 & -m_Z s_W \cos\beta & m_Z s_W \sin\beta \\ * & M_2 & m_Z c_W \cos\beta & -m_Z c_W \sin\beta \\ * & * & 0 & -\mu \\ * & * & * & 0 \end{pmatrix}. \quad (19)$$

Imposing the decoupling limit on the Higgs sector and the neutralino sector by $|\mu|, M_1 >> M_2, m_Z$ simultaneously, leads to a wino-like DM with mass $m_{\chi_1^0} \simeq M_2$ and reduced effective coupling coefficients c_h and c_z [35-37],

$$c_{h\bar{\chi}\chi} \simeq \frac{g}{4}\cos\theta_W \frac{m_Z}{\mu}\left(\frac{m_{\chi_1^0}}{\mu} + \sin 2\beta\right),$$
$$c_{z\bar{\chi}\chi} \simeq -\frac{g}{4}\cos\theta_W \frac{m_Z^2}{\mu^2}\left(1 - \frac{m_{\chi_1^0}^2}{\mu^2}\right), \quad (20)$$

respectively. On the other hand, imposing a different decoupling limit $|\mu|, M_2 >> M_1, m_Z$, we obtain a bino-like DM with mass $m_{\chi_1^0} \simeq M_1$ and

$$c_{h\bar{\chi}\chi} \simeq \frac{g}{4}\sin\theta_W \frac{m_Z}{\mu}\left(\frac{m_{\chi_1^0}}{\mu} + \sin 2\beta\right),$$
$$c_{z\bar{\chi}\chi} \simeq -\frac{g}{4}\sin\theta_W \frac{m_Z^2}{\mu^2}\left(1 - \frac{m_{\chi_1^0}^2}{\mu^2}\right). \quad (21)$$

Both decoupling limits yield a light chargino $\tilde{\chi}^\pm$ with a mass slightly larger than DM mass. For the bino-like DM, the modification to the DM annihilation cross section can be ignored, whereas for the wino-like DM, the correction due to chargino-exchanging DM annihilation into W^+W^- is small[1)], apart from a large contribution of co-annihilation, which occurs in the DM mass range above ~1 TeV [38]. For the decoupling limit, $|c_z| < 1.0\times10^{-3}$ in Eq. (20)-Eq. (21), given $|m_{\chi_1^0}/\mu| \leqslant 0.1$ and $m_Z/|\mu| \leqslant 0.1$. From the contours of the DM relic density in Fig. 2, one finds that the wino-like DM with DM mass below 1 TeV is excluded, which is consistent with the concrete estimate of the wino-like DM mass in Ref. [38].

5 Conclusion

In this paper, we have revisited the Majorana DM, a weakly interacting massive particle, from the viewpoint of the minimal effective field theory. Unlike the Dirac-type analogy, there is no vector coupling between the Majorana DM and Z boson. In this framework, there are only three parameters, i.e., the DM mass and the Yukawa coupling constants c_h and c_Z. Accordingly, it is sufficient to constrain the parameter space in a relatively model-independent way. In order to achieve this, an analytical derivation of DM annihilation into all possible SM final states was performed, which included contributions such as the interference effects and the SM Higgs self-interaction. The fit to the latest LUX, PandaX-II and Xenon-1T limits points to a DM mass lower bound of about ~155 GeV. Also, preliminary applications to the singlet-doublet and MSSM have been addressed. In the singlet-

1) Although kinetically allowed, the ratio between s-wave contribution to DM annihilation due to W^+W^- and top quark final states is of order $\sim m_Z^4/m_\chi^2 m_t^2$, where m_t is the top quark mass. Thus, the s-wave of chargino-exchanging W bosons final states is subdominant in compared with that of top quark final states in DM mass range $m_\chi > m_t$.

doublet model, we found that the singlet-like DM with a mass range between 200 GeV and 600 GeV still survives the latest DM direct detection limits. In the MSSM with decoupled mass spectrum, we recovered the exclusion limits for the neutralino DM mass, such as the wino-like DM.

References

1 G. Jungman, M. Kamionkowski, and K. Griest, Phys. Rept., **267**: 195 (1996), arXiv:hepph/9506380
2 R. Mahbubani and L. Senatore, Phys. Rev. D, **73**: 043510 (2006), arXiv:hep-ph/0510064
3 F. D 'Eramo, Phys. Rev. D, **76**: 083522 (2007), arXiv:0705.4493[hep-ph]
4 R. Enberg, P. J. Fox, L. J. Hall, A. Y. Papaioannou, and M. Papucci, JHEP, **0711**: 014 (2007), arXiv:0706.0918[hepph]
5 T. Cohen, J. Kearney, A. Pierce, and D. Tucker-Smith, Phys. Rev. D, **85**: 075003 (2012), arXiv:1109.2604[hep-ph]
6 C. Cheung and D. Sanford, JCAP, **1402**: 011 (2014), arXiv:1311.5896[hep-ph]
7 L. Calibbi, A. Mariotti, and P. Tziveloglou, JHEP, **1510**: 116 (2015), arXiv:1505.03867[hep-ph]
8 S. Banerjee, S. Matsumoto, K. Mukaida, and Y. L. S. Tsai, JHEP, **1611**: 070 (2016), arXiv:1603.07387[hep-ph]
9 Q. F. Xiang, X. J. Bi, P. F. Yin, and Z. H. Yu, arXiv:1707.03094[hep-ph]
10 Y. G. Kim and K. Y. Lee, Phys. Rev. D, **75**: 115012 (2007), arXiv:hep-ph/0611069
11 S. Kanemura, S. Matsumoto, T. Nabeshima, and N. Okada, Phys. Rev. D, **82**: 055026 (2010), arXiv:1005.5651[hep-ph]
12 A. Djouadi, O. Lebedev, Y. Mambrini, and J. Quevillon, Phys. Lett. B, **709**: 65 (2012), arXiv:1112.3299[hep-ph]
13 L. Lopez-Honorez, T. Schwetz, and J. Zupan, Phys. Lett. B, **716**: 179 (2012), arXiv:1203.2064[hep-ph]
14 A. De Simone, G. F. Giudice, and A. Strumia, JHEP, **1406**: 081 (2014), arXiv:1402.6287[hep-ph]
15 A. Alves, A. Berlin, S. Profumo, and F. S. Queiroz, JHEP, **1510**: 076 (2015), arXiv:1506.06767[hep-ph]
16 M. Escudero, A. Berlin, D. Hooper, and M. X. Lin, JCAP, **1612**: 029 (2016), arXiv:1609.09079[hep-ph]
17 J. Kearney, N. Orlofsky, and A. Pierce, Phys. Rev. D, **95**(3): 035020 (2017), arXiv:1611.05048[hep-ph]
18 A. Alves, G. Arcadi, Y. Mambrini, S. Profumo, and F. S. Queiroz, JHEP, **1704**: 164 (2017), arXiv:1612.07282[hepph]
19 G. Arcadi, M. D. Campos, M. Lindner, A. Masiero, and F. S. Queiroz, arXiv:1708.00890 [hep-ph]
20 S. Matsumoto, S. Mukhopadhyay, and Y. L. S. Tsai, JHEP, **1410**: 155 (2014), arXiv:1407.1859[hep-ph]
21 M. Drees and M. M. Nojiri, Phys. Rev. D, **47**: 376 (1993), arXiv:hepph/9207234
22 G. Belanger, F. Boudjema, A. Pukhov and A. Semenov, Comput. Phys. Commun., **192**: 322 (Comput. Phys. Commun.), arXiv:1407.6129 [hepph]
23 A. Basirnia, S. Macaluso and D. Shih, JHEP, **1703**: 073 (2017), arXiv:1605.08442[hep-ph]
24 P. Batra, A. Delgado, D. E. Kaplan and T. M. P. Tait, JHEP, **0402**: 043 (2004), arXiv:hep-ph/0309149
25 P. A. R. Ade et al (Planck Collaboration), Astron. Astrophys., **571**: A16 (2014), arXiv:1303.5076[astro-ph.CO]
26 X. Cui et al (PandaX-II Collaboration), Phys. Rev. Lett., **119**(18): 181302 (2017), arXiv:1708.06917[astro-ph.CO]
27 E. Aprile et al (XENON Collaboration), Phys. Rev. Lett., **119**(18): 181301 (2017), arXiv:1705.06655[astro-ph.CO]
28 D. S. Akerib et al (LUX Collaboration), Phys. Rev. Lett., **118**(2): 021303 (2017), arXiv:1608.07648[astro-ph.CO]
29 (CMS Collaboration), CMS-PAS-EXO-12-048.
30 V. Khachatryan et al (CMS Collaboration), Eur. Phys. J. C, **75**(5): 235 (2015), arXiv:1408.3583[hep-ex]
31 M. Aaboud et al (ATLAS Collaboration), Phys. Rev. D, **94**(3): 032005 (2016), arXiv:1604.07773[hep-ex]
32 M. Ackermann et al (Fermi-LAT Collaboration), Phys. Rev. D, **88**: 082002 (2013), arXiv:1305.5597[astro-ph.HE]
33 M. Ackermann et al (Fermi-LAT Collaboration), Phys. Rev. D, **91**(12): 122002 (2015), arXiv:1506.00013[astro-ph.HE]
34 M. Ackermann et al (Fermi-LAT Collaboration), Phys. Rev. Lett., **115**(23): 231301 (2015), arXiv:1503.02641[astroph.HE]
35 G. Belanger, F. Boudjema, C. Hugonie, A. Pukhov, and A. Semenov, JCAP, **0509**: 001 (2005), arXiv:hep-ph/0505142
36 M. Badziak, M. Olechowski, and P. Szczerbiak, JHEP, **1603**: 179 (2016), arXiv:1512.02472[hep-ph]
37 M. Badziak, A. Delgado, M. Olechowski, S. Pokorski, and K. Sakurai, JHEP, **1511**: 053 (2015), arXiv:1506.07177[hepph]
38 J. Hisano, S. Matsumoto, M. Nagai, O. Saito, and M. Senami, Phys. Lett. B, **646**: 34 (2007), arXiv:hep-ph/0610249